BEAM INSTRUMENTATION IN J-PARC

T. Toyama[#] and the J-PARC beam instrumentation group,
J-PARC/KEK, 2-4 Shirane Shirakata, Tokai-mura, Naka-gun, Ibaraki, Japan
and 1-1 Oho, Tsukuba, Ibaraki, Japan

Abstract

High intensity protons of $1\text{-}2\times10^{13}$ protons per bunch have been accelerated in the J-PARC accelerators. To meet with the requirements of the high intensity beam diagnostics, we prepare several measures against high intensity proton related issues. The following subjects are reported among many subjects: the coupling impedance reduction of BPMs, a bunch-by-bunch transverse feedback system, a radiation-hard material for the "multi-ribbon profile monitor", and beam-based characterization of the BPM, DCCT and BLM. A big earthquake occurred on May 11, 2011. Its influence on the J-PARC facility is mentioned, although still partially under investigation.

OVERVIEW

J-PARC (Japan Proton Accelerator Research Complex) comprises the 181 MeV linac, the 3 GeV RCS (Rapid-cycling Synchrotron), the 30 GeV (at phase-I) MR (Main Ring) and related experimental facilities. The beam powers have been achieved 120kW at the RCS and 145 kW at the MR with the linac current of 15 mA in recent operations [1]. The goal at each stage is 50 mA at the linac, 1 MW at the RCS and 750 kW or more at the MR. The beam sizes are relatively large comparing to the e+, e- accelerators and high energy proton accelerators. Here are brief estimates of the beam size related quantities: the horizontal and vertical emittances and bunch lengths are ~ 0.1 ns and 0.1 π mmmrad at the linac, 50 - 500 ns and 50 - 200 π mmmrad at the RCS, and 40 - 400 ns and 1 - 50 π mmmrad at the MR, respectively. To accommodate such a beam, the beam instruments are prepared as shown in Fig. 1 [2]. Additional instruments are in preparation to meet with the linac energy and intensity upgrade to 400 MeV and 50 mA [3]. Two bunch shape monitors will be installed at the ACS linac in collaboration with INR.
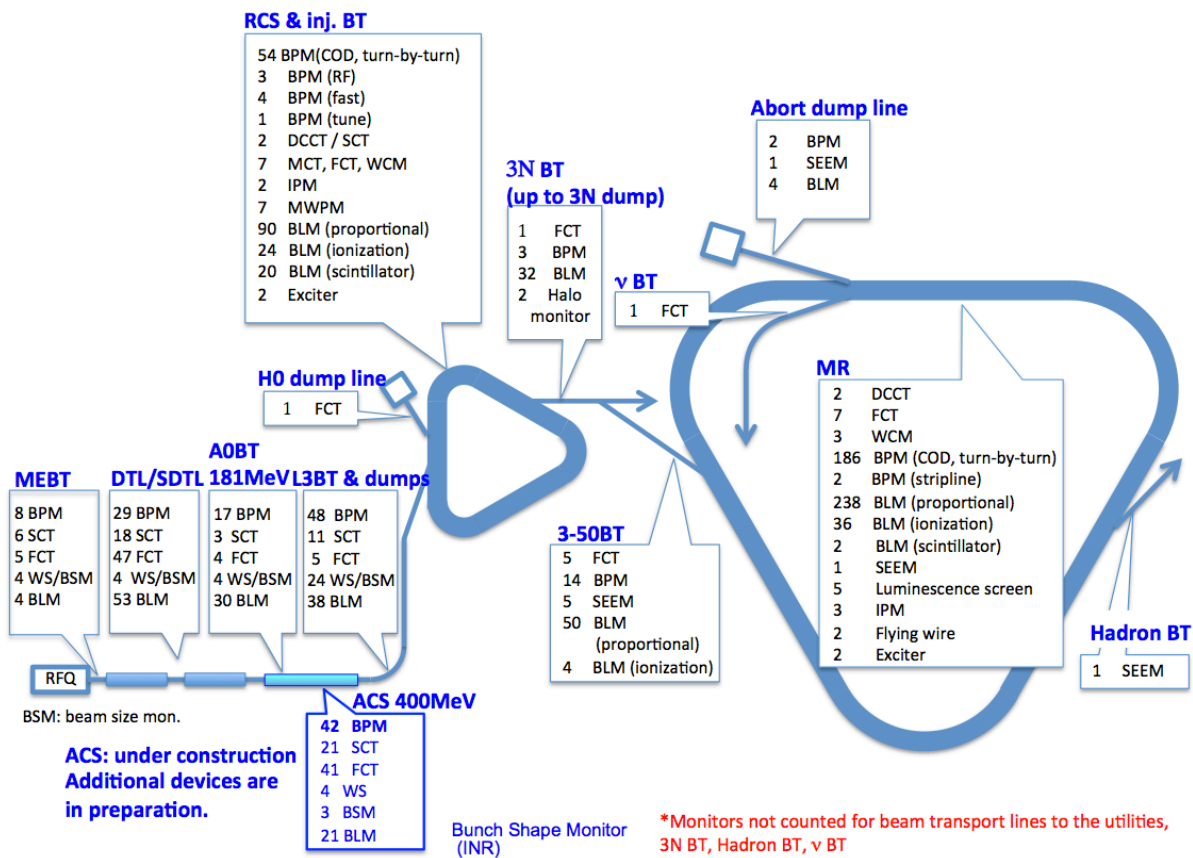

Figure 1: Layout of the beam instruments in the J-PARC accelerators.

[#]takeshi.toyama@kek.jp

BEAM INSTABILITY ISSUES

The beam instabilities become more important as the beam intensity gets larger. Two subjects are picked up here: the BPM design and the transverse feedback damper.

BPM Impedance

The KEK 12GeV-PS had encountered the longitudinal microwave instability in the course of intensity upgrade for the K2K long-baseline ν oscillation experiment in the late 1990s. One of the impedance sources was identified to be the BPMs that employed wall current pickups. The coupling-impedance measurement with a coaxial transmission-line revealed the resonances at ~ 600 MHz and ~ 1.4 GHz. Simulation with "MAFIA" also agreed with the measurement [4].

The longitudinal impedance may be reduced with a larger capacitance. This is qualitatively understood observing the following formula [5],

$$Z_L = \frac{1}{2}\left(\frac{\omega l_0}{\beta c}\right)^2 \frac{R_L}{1 + j\omega C R_L}. \qquad (1)$$

Actually the improved BPM with large capacitance (electrostatic type) showed no detectable resonance (Fig.2) [6]. We keep the same direction in J-PARC, although the electrode shape has been changed to diagonal-cut to obtain a linear position response.
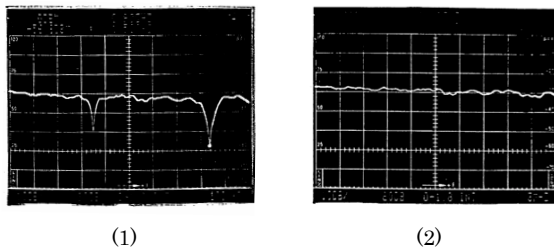

(1)   (2)

Figure 2: Transmissions of the BPM measured with a coaxial transmission line: (1) the previous BPM (WCM type), (2) the improved BPM (ESM type).
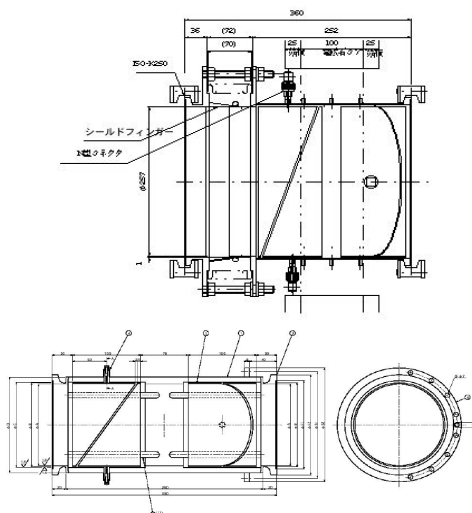

Figure 3: BPMs for the RCS and MR in J-PARC.

The gap size between the electrodes and pipe wall are 2 mm at the RCS- and 1 mm at the MR-BPMs (Fig. 3).

The resulting longitudinal impedance Z_L measured with the stretched wire method [7] has no detectable resonances up to the cut-off frequency, 1.95 GHz [Fig. 5]. The simulation with CST particle studio [8] shows a consistent result (Fig. 6). If $|Z_L/n|$ = 0.35 mΩ, the total of 186 BPMs amounts to 65 mΩ which is much less than the Keil-Schnell criterion for the MR, 9 Ω (max.) [9].
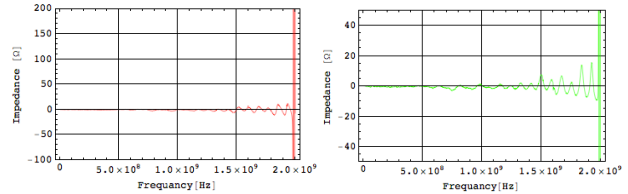

Figure 4: Measured Z_L of the MR BPM. Red and green curves are the real and imaginary impedance, respectively.
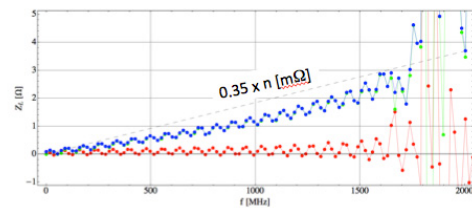

Figure 5: Simulated Z_L of the MR BPM. Red and blue curves are the real and imaginary impedance, respectively. Dashed line indicates Z_L/n = 0.35 mΩ.

Transverse Bunch-by-bunch Feedback

The transverse instability is inevitable in the MR, which may be caused by the resistive wall and kicker magnets [10]. As a measure against this instability, a bunch-by-bunch (B×B) feedback system has been developed [11]. It comprises the diagonal-cut BPM, an analog pre-processing circuit (amplifier/attenuator, LPF), a digital processing circuit (ADC, FPGA, DAC), power amplifiers and a stripline kicker. At the present beam intensity of ~ 10^{13} protons per bunch and small negative chromaticities, horizontal instabilities occur at the MR injection and during acceleration (Fig. 6). Both instabilities are successfully damped with the feedback (Figs. 7 and 8). Routine operation at the beam power of 145 kW with minimum loss is achieved with compromise between the chromaticities optimum and the feedback optimum.
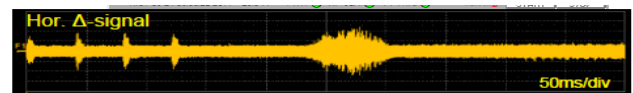

Figure 6: Observed instabilities without the feedback. Four spikes at the beginning are mainly due to kicker error. Broad growth at the middle is due to collective instability.
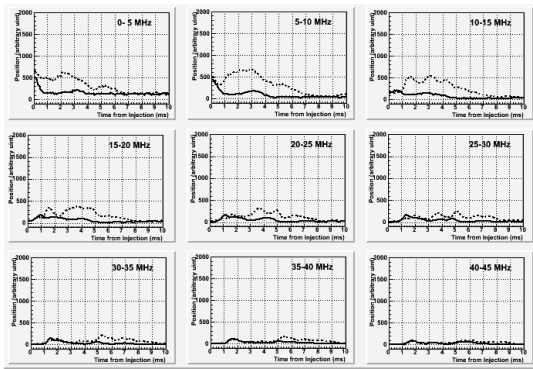
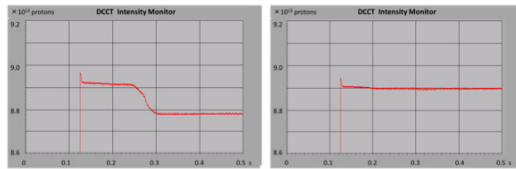Figure 7: Coherent oscillation at the MR injection. Dashed and solid curves are without and with feedback.

Figure 8: The beam loss due to the instability during the MR acceleration. Left and right figures are without and with feedback.

RADIATION-HARD DETECTOR

Requirements on radiation hardness get higher in the high intensity accelerators. Destructive monitors become challenging because material itself should survive, and beam loss small. We have developed the profile monitor for one-pass beamlines fulfilling the above requirements.

Profile Monitors in the J-PARC Accelerators

Prior to describing the multi-ribbon profile monitor, beam profile monitors in J-PARC are summarized. In the linac wire scanners with tungsten wires (ϕ 50 - 80 μm) are installed [12]. Multi-wire profile monitors (MWPM) with tungsten wires (ϕ 100 μm) are installed at the RCS injection section [13]. Ionization profile monitors are installed in the RCS and MR [14]. Flying wire profile monitors with a ϕ7mm carbon wire are installed in the MR [15]. At the 3-50BT, the MR injection section and the hadron BT, MWPMs were installed in the early stage of the beam commissioning. Recently those monitors are replaced by the "multi-ribbon profile monitors" made of a thin graphite sheet (Fig 9).[16]

Multi-ribbon Profile Monitor (MRPM)

The main properties of our graphite are: thickness 2 μm (typical), firing temperature 2600 °C, and the maximum size manufactured 160×320 mm^2. The robustness of the foil against beam impact was investigated by two types of beam tests. The first was a long-run test in which beams hit the target foil during a net 11 months of running. The total proton hit number amounted to more than 5×10^{20}, nevertheless the foil survived. The second was a high-heat

loading test in which the temperature was maintained at 1400 °C with a continuous beam. After 67 min, the foil was broken at the beam spot. On the other hands temperature rise at the target with 3 GeV 4×10^{13} proton beams is estimated to be 200 °C, which is well below the above result. These results show that graphite has high endurance under high beam impact and high heat loading.

As the measurement precision of profiles is determined by ribbon size accuracy and surface uniformity, they are strictly controlled. The evaluation by the 6MeV/n C^{6+} beam (NIRS) showed the difference in emission rate sufficiently less than 1%.

At high intensity beams the space charge effect on emitted dense electrons becomes significant. Secondary electron yields as the function of bias voltages are measured with two beam intensities, 4×10^{11} and 10^{13} ppb, at 3-50BT (Fig.10). The plateau was obtained over the sufficient bias voltage, 70 and 200 V, respectively.

The beam of 1×10^{13} ppb that corresponds to beam power of 100 kW was successfully measured (Fig. 11).
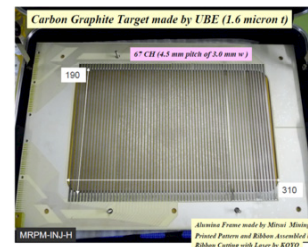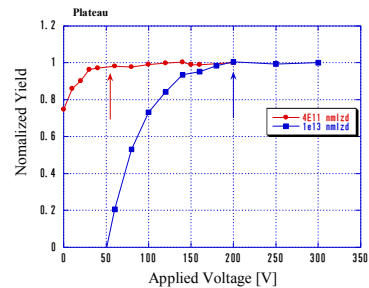

Figure 9: MRPM with the laser-cut graphite sheet.

Figure 10: Normalized secondary electron yields as the function of bias voltages.
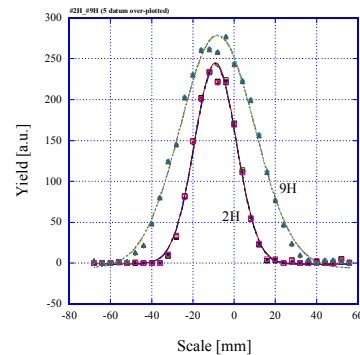

Figure 11: Measured beam profiles at 1×10^{13} ppb.

BEAM-BASED CHARACTERIZATION

Beam-based Alignment (BBA) of BPMs

Beam-based alignment of BPMs is one of the standard calibration techniques. A certain BPM offset position is calibrated varying the focusing strength of the neighbouring quadrupole magnet (QM). In the RCS, however, the QMs are energized only in series connection within a certain QM family. Therefore the conventional BBA algorithm, in which one BPM is calibrated with one QM, is extended to that multiple BPMs calibrated with multiple QMs, and successfully applied to the RCS (Fig.12) [17]. To confirm the algorithm the conventional one is compared to the new one in the MR where the QM can be energized both individually and in the family. A small discrepancy ~100 μm exists between the results from both algorithms in the vertical plane [17] and under further investigation.
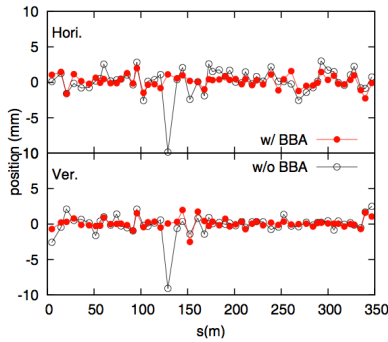

Figure 12: COD correction without (open circle) and with (closed circle) using BBA results. Upper is for horizontal and lower is vertical one. The COD correction was improved using the BBA results.

Beam-based Gain Calibration BPMs

In KEKB, we found noticeable errors larger than 0.1mm in the almost all BPM readings. These errors come from the gain imbalance among 4 output voltages of a BPM. The gain imbalance is considered to come from the imbalance of the signal transmission in the cables and processing circuit gains. By this reason the gains of every BPMs of KEKB have been calibrated by a non-linear chi-square method. The same algorithm cannot apply to the J-PARC BPM because the KEKB BPMs are button-type on the other hands the J-PARC ones are diagonal-cut-type.

Using the BPM linear position response,

$$V_{L,j} = g_L \lambda_j \left(1 + \frac{x_j}{a}\right), \quad V_{U,j} = g_U \lambda_j \left(1 + \frac{y_j}{a}\right),$$
$$V_{R,j} = g_R \lambda_j \left(1 - \frac{x_j}{a}\right), \quad V_{D,j} = g_D \lambda_j \left(1 - \frac{y_j}{a}\right), \quad (2)$$

for the j-th measurement, the following relation is reduced

$$\frac{V_{L,j}}{g_L} - \frac{V_{R,j}}{g_R} = \frac{V_{U,j}}{g_U} - \frac{V_{D,j}}{g_D}, \quad (3)$$

Setting $g_L = 1$ and executing measurements more than 3 times, we can solve simultaneous linear equations of Eq (3) with total least squares algorithm [18]. The method looks promising.

Correction of DCCT Response

In high intensity accelerators of beam intensities above ~10^{13} particles per pulse, beam losses even in the order of 0.1 % are issues due to its residual activations. A beam DCCT may be very useful if it can detect such beam losses. The DCCT in the J-PARC MR has an enough resolution for such purpose [19]. But so far three systematic relative errors are observed in the order of 0.1 %; the deviation in the step response, the effect of synchrotron oscillation and the magnetic leakage field effect. Among these the deviation in the step response is corrected [20]. At first the DCCT system was modeled using the response to the fast beam extraction. Then digital filter parameters for correction were calculated with the model, and applied to the DCCT output signal (Fig. 13). The relative deviation is corrected within 0.1% (Fig. 14).
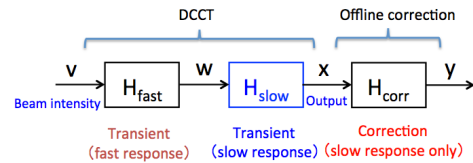

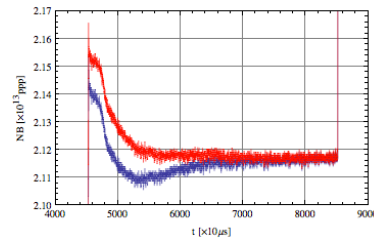Figure 13: Block diagram of the DCCT and corrector.

Figure 14: Measured (dark-blue curve) and corrected (red curve) beam intensities.

Calibration of BLM Sensitivity

To estimate slow extraction (SX) inefficiency, beam-based calibrations of the BLMs of the SX straight section were made [21]. The SX involves localized beam losses at an electrostatic septum and at a magnetic septum, and beam loss signal distribution is peeked at BLM#76 and BLM#82. A local bump orbit was made to reproduce a beam loss at the electrostatic septum and at the magnetic septum. The beam energy was 30GeV and the bias voltage was set to 1.3kV. Output charges are shown in fig. 6 as a function of the beam loss intensity measured by using a MR DCCT. The SX inefficiency is estimated using these calibration curves with the resolution of ~0.1%.
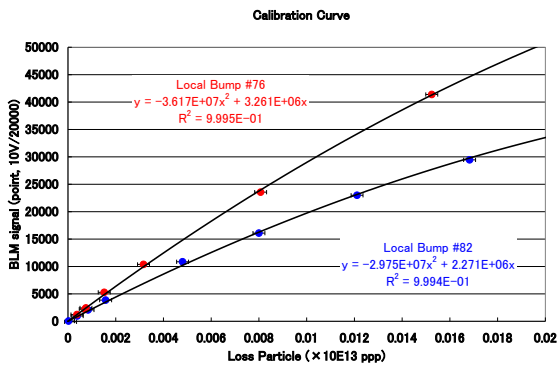
Figure 15: BLM response to the beam loss at the electrostatic septum (local bump #76) and at the magnetic septum (local bump #82).

BLMs in the J-PARC Accelerators

The BLMs in the J-PARC comprises mainly proportional counters (p-BLM) and additionally scintillator and photomultiplier (PMT) pairs, and air ionization chambers. The p-BLMs have suffered from the X-ray background of the S-DTL RF cavities in the linac section. Recently scintillator and PMT pairs successfully detect the linac beam loss without X-ray background [22]. In the MR air ionization chambers of 1 meter long will be added and complement the p-BLM. Utility of fast response detectors as a scintillator and PMT pair, SSD or diamond in the MR is now under consideration.

INFLUENCE OF THE 3.11 EARTHQUAKE

The great earthquake occurred on March 11, 2011 at 14:46 JST off the Pacific coast of Tohoku. The seismic intensity was 6⁻ (JMA scale) at J-PARC [23]. Although tsunami came to the Tokai-site coast, well below the ground level of J-PARC. No injuries are observed for J-PARC related persons. Tsunami height at the Tokai-site seems to be TP 4 - 5 m [24], not far from the hazard map [25].

Alignments of the accelerators in J-PARC were deformed. Vertical level variation of ~40 mm was observed in the linac and ~8 mm in the MR. Detailed survey is under way [26].

Beam instruments also suffered from the great quakes. The biggest damages occurred in the linac [27]. Brazing between the ceramic tube and SS vacuum pipe of the FCTs was detached. Some bellows were broken. There observed no serious damages in the RCS and MR.

The recovery schedule is announced in [28].

CONCLUSION

Measures against high intensity proton beams have been taken: low impedance diagonal-cut BPMs, a transverse B×B feedback damper and rad-hard SEM with multi-ribbon of graphite were installed and work successfully. Precisions have been enhanced with beam-based characterization: the BBA of BPMs with multiple-

BPMs by family-QM, BPM gain calibration, DCCT response correction and BLM sensitivity calibration.

ACKNOWLEDGEMENTS

The authors would like to thank all the J-PARC crew who have helped the J-PARC beam instruments development and operation.

REFERENCES

[1] T. Koseki et al., Proc. of HB2010, p.16.
[2] S. Lee *et al.*, Proc. of LINAC2004, p.441, Hayashi *et al.*, Proc. of EPAC2008, p.1125, T. Toyama *et al.* Proc. of PAC2009, p.1964. The number of BPMs at the linac is determined necessary and sufficient for beam tuning. The RFQ is optimized using the downstream SCT. The RF amplitude is adjusted untill the relative beam transmission and the simulation results agree each other.
[3] A. Miura *et al.*, in these proceedings, Miyao *et al.*, ibid.
[4] K. Takayama *et al.*, Phys. Rev. Lett. 78 (1997) 871.
[5] Zotter, Kheifets, "Impedances and Wakes in High-Energy Particle Accelerators".
[6] D. Arakawa, Proc. of the meeting on the technical study at KEK, KEK-Proceedings-98-1, p.1 (*Japanese*).
[7] F. Caspers, in "Handbook of Accelerator Physics and Engineering", World Scientific (1999), A. Chao and M. Tigner (Eds.).
[8] CST particle studio, http://www.cst.com.
[9] Y. Shobuda, in High Energy Accelerator Seminor OHO'10 (*Japanese*).
[10] Y.H.Chin *et al.,* Proc. of HB2008, p.40.
[11] Y. Kurimoto *et al.*, in these proceedings.
[12] H. Akikawa *et al.*, Proc. of PAC07, p.1472.
[13] S. Hiroki *et al.*, Proc. of EPAC2008, p. 1131.
[14] K. Satou *et al.*, Proc. of HB2010, p.506.
[15] S. Igarashi *et al.*, to be presented at IPAC'12.
[16] Y. Hashimoto *et al.*, Proc. of HB2010.
[17] N. Hayashi *et al.*, Proc. of HB2010.
[18] M. Tejima *et al.*, in these proceedings.
[19] Y. Hashimoto *et al.*, to be presented at the 8th ann. meeting of Part. Accel. Society of Japan (*Japanese*).
[20] T. Toyama *et al.*, ibid.
[21] K. Satou *et al.*, Proc. of IPAC'10, p. 990.
[22] A. Miura *et al.*, in these proceedings.
[23] Japan Meteological Agency, http://www.seisvol.kishou.go.jp/eq/shindo_db/db_map/indexemg.html (*Japanese*).
[24] Earthquake research institute, the Univ. of Tokyo, http://outreach.eri.u-tokyo.ac.jp/eqvolc/201103_tohoku/eng.
[25] Ibaraki prefectural goverment, http://www.pref.ibaraki.jp/bukyoku/doboku/01class/class06/tsunami/ (*Japanese*).
[26] M. Shirakata *et al.*, to be presented at IPAC'12.
[27] A. Miura *et al.*, to be presented at IPAC'12.
[28] S. Nagamiya, http://j-parc.jp/en/topics/2011/en.html #Recovery_schedule.